Acta histochemica 111 (2009) 15—24

Available online at www.sciencedirect.com
ScienceDirect

acta histochemica
www.elsevier.de/acthis

Nitric oxide production during the osteogenic differentiation of human periodontal ligament mesenchymal stem cells

Monia Orciani[a], Oriana Trubiani[b], Arianna Vignini[c], Monica Mattioli-Belmonte[a], R. Di Primio[a], Eleonora Salvolini[a,*]

[a]*Dipartimento di Patologia Molecolare e Terapie Innovative—Istologia, Università Politecnica delle Marche, Via Tronto 10/A, 60020 Ancona, Italy*
[b]*Dipartimento di Scienze Odontostomatologiche, Università di Chieti-Pescara Via Vestini 31, 66100 Chieti, Italy*
[c]*Istituto di Biochimica, Università Politecnica delle Marche, Via Tronto 10/A, 60020 Ancona, Italy*

Received 28 November 2007; received in revised form 8 February 2008; accepted 19 February 2008

KEYWORDS
Mesenchymal stem cells;
Periodontal ligament;
Osteogenesis;
Nitric oxide;
Intracellular calcium

Abstract

The critical tissues that require regeneration in the periodontium are of mesenchymal origin; therefore, the ability to identify, characterize and manipulate mesenchymal stem cells within the periodontium is of considerable clinical significance. In particular, recent findings suggest that periodontal ligament cells may possess many osteoblast-like properties. In the present study, periodontal ligament mesenchymal stem cells obtained from healthy volunteers were maintained in culture until confluence and then induced to osteogenic differentiation. Intracellular calcium ($[Ca^{2+}]_i$) concentration and nitric oxide, important signalling molecules in the bone, were measured along with cell differentiation. Alkaline phosphatase activity was assayed and bone nodule-like structures were evaluated by means of morphological and histochemical analysis. Our results showed that the periodontal ligament mesenchymal stem cells underwent an *in vitro* osteogenic differentiation, resulting in the appearance of active osteoblast-like cells together with the formation of calcified deposits. Differentiating cells were also characterized by an increase of $[Ca^{2+}]_i$ and nitric oxide production. In conclusion, our data show a link between nitric oxide and the osteogenic differentiation of human periodontal ligament mesenchymal stem cells, thus suggesting that local reimplantation of expanded cells in conjugation with a nitric oxide donor could represent a promising method for treatment of periodontal defects.

*Corresponding author. Tel./fax: +39 071 2206078.
E-mail address: e.salvolini@univpm.it (E. Salvolini).

0065-1281/$ - see front matter © 2008 Elsevier GmbH. All rights reserved.
doi:10.1016/j.acthis.2008.02.005

Introduction

Mesenchymal stem cells (MSCs), precursors of mesenchymal tissues, are multipotent and represent the precursors for bone, cartilage, muscles and connective tissue (Jiang et al., 2002). Several studies have demonstrated that MSCs expanded *ex vivo* are not only able to regenerate tissues of mesenchymal lineage, but also to differentiate into cells derived from other embryonic layers, including neurons (Crevensten et al., 2004; Chamberlain et al., 2004; Grinnemo et al., 2004; Sugaya, 2003). Owing to these characteristics, MSCs are good candidates for treatment of mesenchymal disorders, gene therapy, transplantation and tissue engineering. Even if bone marrow represents a well-established source of MSCs, these cells could also be obtained in large quantities with minimal surgical stress from a variety of tissues and organs, such as umbilical cord, circulating blood, dental pulp, periodontal ligament (PDL), etc. (Prockop, 1997; Gage, 2000; Spradling et al., 2001; Toma et al., 2001; Pierdomenico et al., 2005; Trubiani et al., 2005; Ivanovski et al., 2006).

The PDL, in particular, represents an interesting and promising stem cell source in adults. The PDL not only has an important role in supporting teeth, but also contributes to tooth nutrition. In addition, the presence of multiple cell types within the PDL has led to speculation that this tissue might contain progenitor cells that maintain tissue homeostasis and regenerate periodontal tissues (Beertsen et al., 1997; Gould et al., 1980; Boyko et al., 1981).

Periodontal diseases are the most frequent cause of tooth loss, owing to the destruction of the tooth-supporting tissues, including PDL, cementum, gingiva and alveolar bone, and consequently the reconstruction of healthy periodontium is a major goal of periodontal therapy. Several new approaches have been developed for treating periodontal defects, including guided tissue regeneration and growth factors, but so far, none of these treatments has provided a consistently predictable outcome. As the critical tissues that require regeneration in the periodontium are of mesenchymal origin, the ability to identify, characterize and manipulate MSCs within the periodontium is of considerable clinical significance, especially in terms of developing novel mechanisms of achieving periodontal regeneration. Regarding, in particular, the alveolar bone repair, previous findings have indicated that PDL cells may possess several osteoblast-like properties, including the ability to form calcified nodules *in vitro* (Morishita et al., 1999; Seo et al., 2004). It is well known that the proliferation and differentiation of mesenchymal cells into the osteoblastic lineage is regulated by an intrinsic genetically defined program, which is controlled by various transcription factors, cytokines, morphogens, and secreted growth factors (Narayanan et al., 2003). Many of these molecules have one thing in common, they are capable of increasing intracellular calcium ($[Ca^{2+}]_i$) by various mechanisms. Several cellular effects of Ca^{2+} are mediated by the Ca^{2+} binding protein, calmodulin (CaM). CaM is involved in almost all aspects of cellular functions via the diversity of its target proteins, which include nitric oxide synthase (NOS) (Zayzafoon, 2006).

Three isoforms of NOS have been identified: a neuronal form (nNOS), an endothelial form (eNOS) and an inducible form (iNOS) (Ralston, 1997). Since their original discovery, it has become clear that the expression of both nNOS and eNOS (the ''constitutive'' isoforms) is not restricted to vessels and neural tissue: both have been observed in tumor cell lines, gut, muscle and in bone-derived cells such as osteoblasts and osteoclasts (Salter et al., 1991; Helfrich et al., 1997). It has been demonstrated that the activity of both eNOS and iNOS is significant in bone biology, although there is a consensus that under physiological conditions eNOS probably represents the major NOS activity regulating bone formation. In fact, it has been suggested that the constitutive nitric oxide (NO) production may exert an autocrine effect on osteoblast growth and function (Riancho et al., 1995).

Usually, when human bone cells are studied, they are most commonly derived from non-dental sites; for this reason, the aim of the present study was to evaluate the osteogenic differentiation of MSCs expanded *ex vivo* from human PDL and their ability to form calcified deposits as previously observed in MSCs derived from bone marrow and dental pulp (Gronthos et al., 2000; Shi and Gronthos, 2003; Donzelli et al., 2007). For this purpose, we monitored the morphological features, the bone nodule arrangement, the alkaline phosphatase activity, the $[Ca^{2+}]_i$ concentration and the NO production of PDL-MSCs obtained under selective cultivation conditions.

Materials and methods

Cell culture

Human PDL was obtained from 10 volunteers aged 20–35 years after informed consent. The study protocol was approved by the Ethics Committee of

the University of Chieti–Pescara. Both systemic and oral diseases were absent in all subjects. The explants were scraped using Gracey's curettes from the alveolar crest and horizontal fibers of PDL attached to the roots of extracted non-carious molar teeth and cultured in MSC growth medium (MSCGM) (Cambrex Company, Walkersville, USA) as previously described (Trubiani et al., 2005).

After 20 days of culture, numerous cells forming colonies (CFU-F) migrated from the explants. At day 7, adherent cells, which were 80–90% confluent, were isolated using 0.25% trypsin-EDTA solution (Sigma-Aldrich, Milan, Italy) and plated in tissue culture polystyrene flasks at 5×10^3 cells/cm^2. Primary cultures of PDL-MSCs mainly consisted of colonies of bipolar fibroblastoid cells, which, after subcultivation, proliferate with a population-doubling time of 48 h, reaching a confluent growth-arrested condition.

Cells in the developing adherent layer were used for the experiments described after removal with trypsin solution and cell growth was evaluated by trypan blue exclusion test.

Flow cytometry analysis

PDL-MSCs cells were washed in phosphate buffered saline (PBS) and then incubated with 2 μg/ml of the following mouse anti-human monoclonal antibodies: fluorescein isothiocyanate (FITC)-conjugated HLA-ABC, HLA-DR, CD10, CD11b, CD14, CD29, CD34, CD44, CD49d, CD73 and phycoerythrin (PE)-labelled CD90, CD105, CD166, for 30 min at 4 °C. All antibodies were purchased from Becton-Dickinson.

The cell suspension was then washed twice with PBS and analyzed on a FACStar plus flow cytometer (Becton-Dickinson, Mountain View, CA, USA).

Osteogenic differentiation

At the 2nd passage, cells were plated on tissue culture polystyrene dishes in osteogenic medium comprising osteogenic supplements (10^{-8} M dexamethasone, 5 mM β-glycerophosphate and 50 μg/ml L-ascorbic acid) (Sigma-Aldrich, Milan, Italy). Control cultures were maintained in MSCGM medium without osteogenic supplements. Cells were re-fed every 2 days and the cultures were maintained until bone nodule-like structures were observed (usually after 4–6 weeks). These nodular aggregates were evaluated by phase contrast microscopy and subsequently prepared for morphological and biochemical analyses.

Light microscopy

Morphological analyses were performed by standard procedures using hematoxylin–eosin staining. Masson's trichrome dye staining was performed by routine protocol and used for examination of the connective tissue and its collagen network.

Histochemistry

As an indicator of mineralization within the PDL-MSC cell cultures induced to osteogenic differentiation, calcium deposition was analyzed by alizarin red S staining with slight modifications to the method previously described by Chaudhary et al. (2004). Briefly, the cells were rinsed twice with PBS and fixed with ice-cold 70% ethanol. After rinsing in deionized water, the plates were stained with 40 mM alizarin red S (Sigma-Aldrich, Milan, Italy) solution, pH 4.2, for at least 10 min, rinsed in water and washed in Tris buffered saline (TBS) for 15 min to remove non-specific stain. The plates were then air dried and analyzed by light microscopy.

Transmission electron microscopy (TEM)

The samples were fixed with 2.5% glutaraldehyde in 0.1 M cacodylate buffer, pH 7.4, for 1 h and post-fixed with 1% OsO_4 in the same buffer for 1 h at 4 °C. They were then stained overnight with saturated aqueous uranyl acetate solution, dehydrated and embedded in Spurr's medium (Polysciences, Warrington, PA, USA). Semi-thin sections were stained with toulidine blue. Thin sections were counterstained with lead citrate. Ultrastructural observations were carried out using a Jeol JEM 1010 transmission electron microscope operating at 60 kV.

Scanning electron microscopy (SEM) and energy dispersive X-ray microanalysis (EDAX)

The samples were prefixed for 4 h at 4 °C in 2% glutaraldehyde in 0.05 M phosphate buffer (pH 7.4), post-fixed in 1% OsO_4, dehydrated in increasing ethanol concentrations and then critical point-dried. They were then mounted on aluminum stubs and gold-coated in an Emitech K 550 (Emitech Ltd. Ashford, Kent, UK) sputter-coater before imaging by means of a SEM (LEO 435 Vp Cambridge, UK). In order to determine the element content, the specimens were examined by means of EDAX. After fixation and dehydration, the samples were dried, sputtered with carbon and observed with an SEM Philips XL 20 (Royal Philips Electronic, Eindhoven,

The Netherlands) equipped for X-ray microanalysis (EDS-PV 9800). Specimens were observed using the secondary electron (SE) detector. The program EDX control was used for collecting spectra and EDX mapping was used for determining elemental distribution.

Alkaline phosphatase (ALP) activity measurement

ALP activity was measured on samples of 100,000 cells, detached by means of trypsin-EDTA solution (Sigma-Aldrich, Milan, Italy) and centrifuged for 10 min at 140*g*. The supernatants were removed and immediately analyzed for alkaline phosphatase activity using an automated colorimetric assay (Roche Diagnostics, Randburg, South Africa), according to manufacturer's instructions. The protein content of the supernatant was analyzed using the Bradford method (Bradford, 1976). Alkaline phosphatase activity was calculated as mU of activity per mg of protein.

Intracellular Ca^{2+} concentration

Intracellular Ca^{2+} concentration was measured in intact cells using the fluorescent probe FURA 2-AM (Sigma-Aldrich, Milan, Italy) as previously described (Grynkiewicz et al., 1985). Determinations were performed using a Perkins-Elmer LS 50 B spectrofluorometer at 37 °C according to the method of Rao (1988). Fluorescence intensity was evaluated at a constant emission wavelength (490 nm) with changes in the excitation wavelength (340 and 380 nm). Calibration was carried out as described by Grynkiewicz et al. (1985) using the equation:

$$[Ca^{2+}]_i = k_d \frac{(R - R_{min})}{(R_{max} - R)} \frac{S_{f2}}{S_{b2}}$$

where K_d is the dissociation constant of the Ca^{2+}–FURA 2 interaction in the cytosolic environment; R is the ratio of the fluorescence intensities at excitation wavelengths 340 and 380 nm; R_{min} and R_{max} are the ratios of the fluorescence intensities without Ca^{2+} and with saturating levels of Ca^{2+}, respectively; S_{f2} and S_{b2} are fluorescence intensities at 380 nm without Ca^{2+} and with saturating levels of Ca^{2+}, respectively. R_{min} and S_{f2} were measured after cellular lysis with 1% Triton X-100 and addition of 10 mM EGTA, pH 8.3. R_{max} and S_{b2} were determined after lysis and addition of $CaCl_2$. Autofluorescence was subtracted prior performing the Ca^{2+} calibration procedure.

Nitric oxide (NO) production

NO released by the cells was measured in the intact cells suspension as nitrite/nitrate, by the Griess reaction (Green et al., 1982). In this assay, equal amounts of 1% sulphanylic acid and 0.1% *N*-(1-naphthyl)ethylene diamine were added to the samples and the resulting absorbance was measured at 543 nm. Blank (background) was determined in each experiment utilizing medium incubated without cells. The amount of NO in each sample was determined using a standard curve generated with known concentrations of NO and expressed as nmol NO/mg protein.

Statistical analysis

All quantitative data were analyzed by the Student *t*-test. The results were presented as means ± standard deviations ($n = 10$). All experiments were performed at least four times. *P* values of less than 0.05 were considered statistically significant.

Results

In this study, a pluripotent stem cell population derived from the alveolar crestal and horizontal fibers of human PDL was isolated. The immunophenotype of these cells, as studied by flow cytometric

Table 1. Flow cytometry results of PDL-MSCs cells labelled for positive (CD29, CD44, CD73, CD90, CD105, CD166, HLA-ABC) and negative (CD10, CD11b, CD14, CD34, CD49d, HLA-DR) mesenchymal markers

Marker	Labelling
CD10	−
CD11b	−
CD14	−
CD29	++
CD34	−
CD44	++
CD49d	−
CD73	++
CD90	++
CD105	+/−
CD166	+
HLA-ABC	++
HLA-DR	−

Positive immunolabelling (+) was defined as the level of fluorescence greater than 80% of the corresponding isotype-matched control antibodies. Percentages less than 2% were considered negative (−), while marker labelling ranged between 15% and 30% was defined as weakly positive (+/−).

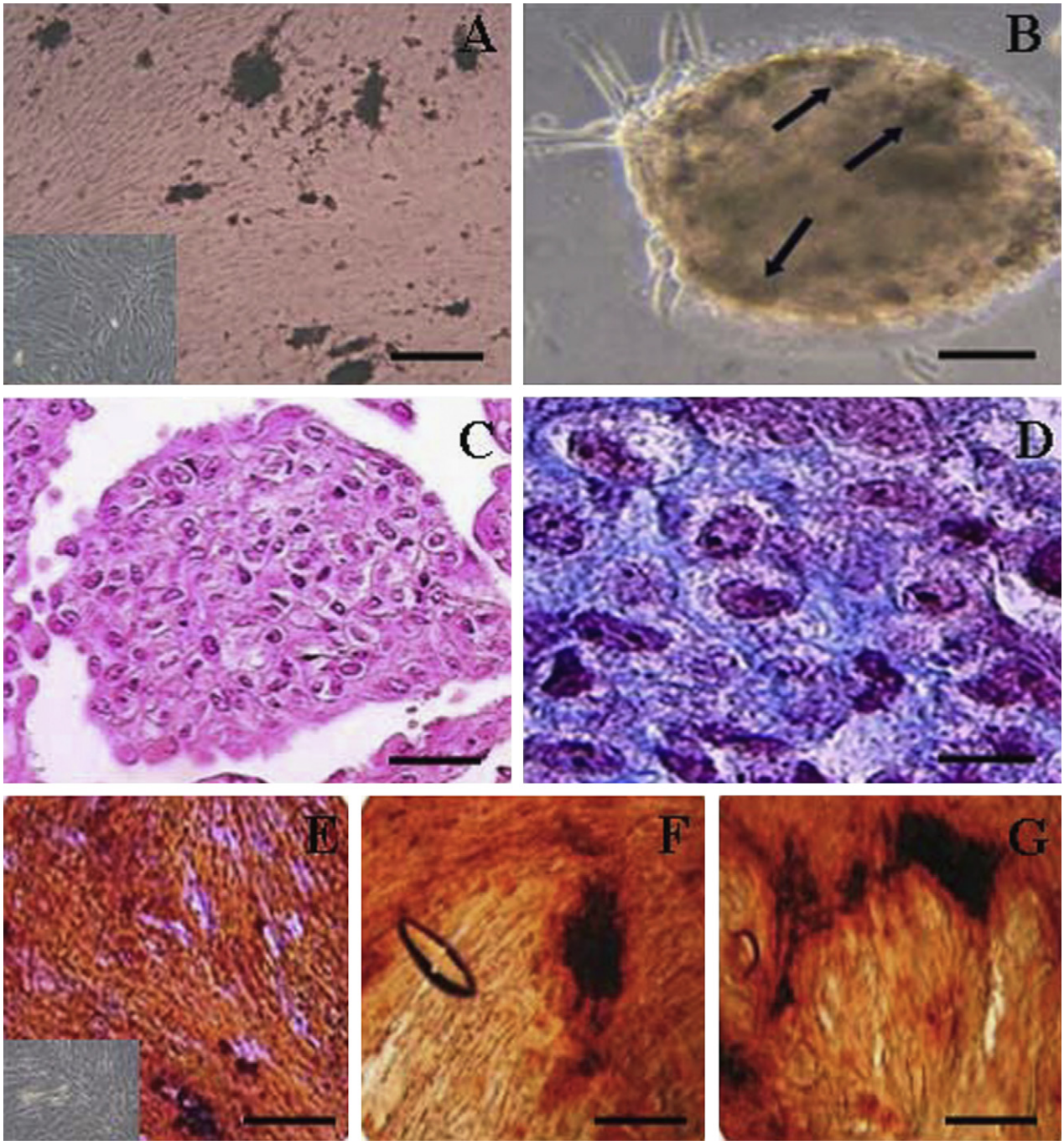

Fig. 1. *Section A*, *inset*: phase contrast microscopy observation of control PDL-MSCs; after 28 days of culture in MSCGM medium alone. The cells do not show any nodular aggregates. *Sections A and B*: phase contrast microscopy observation of differentiating living PDL-MSCs cells, at low and high magnification, respectively. Several cellular aggregates are present, many of which display a bone nodule-like organization (arrows). *Section C*: hematoxylin and eosin staining, detailing the high cellularity of these aggregates. The cells, as revealed by the Masson's trichrome staining (*Section D*), synthesize an abundant extracellular matrix, with the presence of collagen fibers (blue). *Sections E–G*: PDL-MSCs stained with alizarin red. The inset represents the cells after 28 days of culture in MSCGM medium alone. *Sections E–G* show the results of osteogenic induction at day 14, 21, and 28, respectively. Alizarin red positive aggregates are already present at day 14 (*Section E*). At days 21 and 28 (*Sections F* and *G*, respectively) positive alizarin red aggregates are larger and stain more intensively. Sections A, and E–G: bar = 500 μm; Sections B and C: bar = 100 μm; Section D: bar = 30 μm.

analysis, disclosed the homogeneous presence of the mesenchymal-related antigens: CD29, CD44, CD73, CD90, CD166, HLA-ABC. PDL-MSCs were negative for: CD10, CD11b, CD14, CD34, CD49d, HLA-DR, while weakly positive for CD105 (Table 1). Therefore, the primary cultured cells derived from the PDL were of mesenchymal type. Among the tissue obtained from the donors, the pattern of cell surface antigen immunolabelling did not vary. These PDL-MSCs were treated for osteogenic differentiation as described for up to 28 days. The osteogenic differentiation was evaluated using morphological and biochemical techniques both in cells grown in osteogenic medium and in cells cultured in MSCGM medium alone, which represented the control cells.

Morphological analysis of PDL-MSCs differentiation, evaluated by light microscopy, is reported in Fig. 1. Control PDL-MSCs did not show any nodular aggregates after 28 days of culture, as revealed by phase contrast microscopy observation (Fig. 1, Section A, inset). On the contrary, the treatment with osteogenic inductors provoked the formation of cell aggregates and production of extracellular matrix with subsequent mineralization. Fig. 1 Sections A and B show, by phase contrast microscopy, the presence of living cells organized in bone nodule-like structures. These structures, stained with hematoxylin and eosin (Fig. 1, Section C), were made up of differently shaped cells, able to produce an extracellular matrix, as revealed by Masson's trichrome staining (Fig. 1, Section D). The nodular aggregates in differentiating cultures stained with alizarin red, demonstrating that the deposits observed are calcified (Fig. 1, Sections E–G). Alizarin red positive aggregates were already present at day 14 (Fig. 1, Section E). At days 21 and 28 (Fig. 1, Sections F and G, respectively) positive alizarin red aggregates were larger and stained more intensely indicating that a more extensive calcium deposition had occurred. Extensive osteogenic differentiation, as evidenced by alizarin red staining, was noticeable only in PDL-MSCs exposed to osteogenic conditions, while no mineralization was observed in the cells cultured in control medium (Fig. 1, Section E, inset).

The semithin sections stained with toluidine blue (Fig. 2, Section A) demonstrate the osteoblast-like cells surrounded by extracellular matrix. In the inset is shown control PDL-MSCs with a fibroblast-like morphology. During osteogenic differentiation

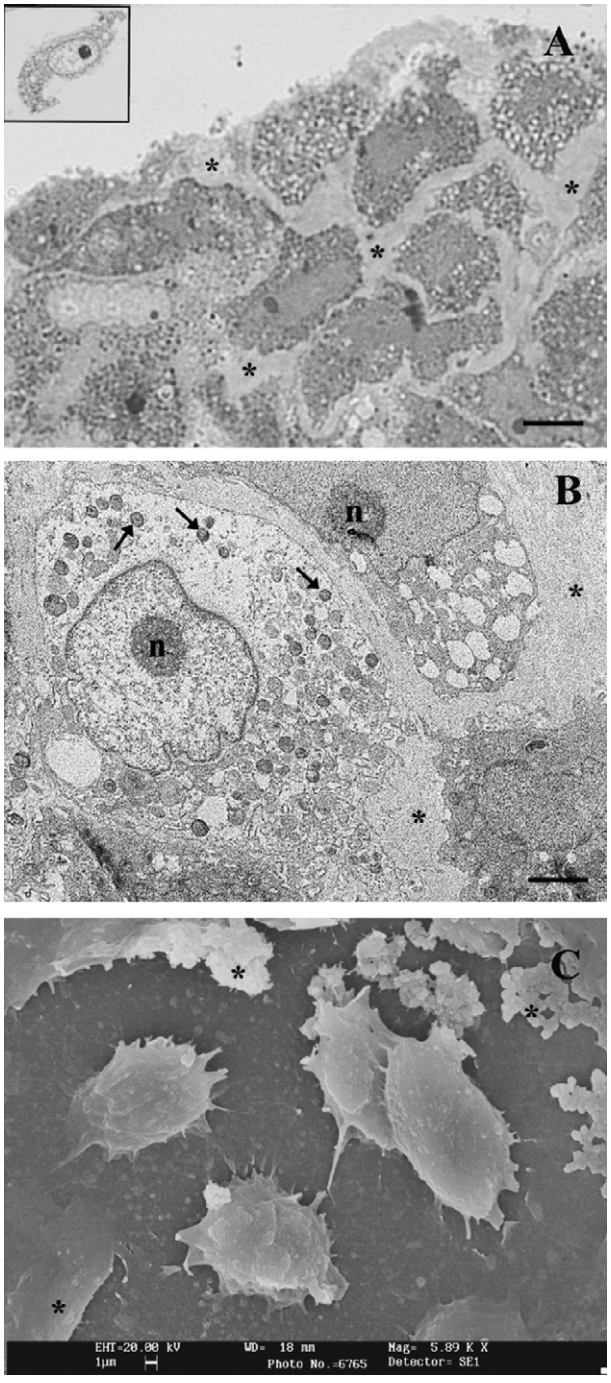

Fig. 2. *Section A*: semithin section observation of osteoblast-like PDL-derived cells, showing differently shaped cells surrounded by extracellular matrix (∗). The insert shows the morphological feature of control PDL-MSC with a typical fibroblast-like appearance. *Section B*: TEM analysis of osteogenic differentiated cells, with large rough endoplasmic reticulum cysternae and numerous mitochondria. n = nucleolus; thin arrows = mitochondria. Section C: SEM analysis, showing the oval shape of osteoblast-like cells, with the presence of short protrusion of the plasma membrane. The cells are surrounded by an abundant extracellular matrix (∗) undergoing an initial mineralization process, evaluated by means of EDAX. Section A: bar = 10 μm; Section B: bar = 2 μm; Section C: bar = 1 μm.

MCSs changed from their characteristic fibroblast-like phenotype towards an osteoblast-like phenotype, showing a typical polygonal appearance.

Electron microscopy analysis permitted viewing of the ultrastructural features of PDL-MSCs induced to osteogenic differentiation. The cells, observed by means of TEM (Fig. 2, Section B), had euchromatic nuclei with prominent nucleoli. In the cytoplasm, numerous mitochondria and cisternae of rough endoplasmic reticulum were seen, both indicating the synthetic activity of these cells involved in the production of extracellular matrix components. The cell plasma membrane showed short protrusions, as confirmed by SEM analysis (Fig. 2, Section C).

The results of the energy dispersive X-ray microanalysis (Fig. 3) showed the presence of mineralized deposits containing calcium and phosphorus in the areas resembling bone-like nodules. ALP activity, a well-known marker of osteoblast differentiation and function at the beginning of mineralization of bone tissue, was significantly higher in the differentiated cells compared to the control cells from day 14 of induction onwards (controls: time $0 = 0.14 \pm 0.01$ mU/mg protein; day $14 = 1.9 \pm 0.1$ mU/mg protein; day $21 = 1.6 \pm 0.3$ mU/mg protein; day $28 = 0.9 \pm 0.09$ mU/mg protein. Differentiated: time $0 = 0.15 \pm 0.03$ mU/mg protein; day $14 = 12.78 \pm 1.07$ mU/mg protein; day $21 = 18.54 \pm 1.65$ mU/mg protein; day $28 = 20.42 \pm 1.98$ mU/mg protein) (Fig. 4).

With regard to the $[Ca^{2+}]_i$, our results reveal that it was significantly lower in the control cells in comparison with the differentiated cells and it increased along with the osteogenic differentiation (controls: time $0 = 35.86 \pm 3.25$ nM; day $14 = 41.73 \pm 5.07$ nM; day $21 = 45.02 \pm 6.34$ nM; day $28 = 39.41 \pm 4.78$ nM. Differentiated: time $0 = 36.49 \pm 4.51$ nM; day $14 = 126.37 \pm 10.41$ nM; day $21 = 167.13 \pm 12.02$ nM; day $28 = 208.55 \pm 15.83$ nM) (Fig. 5). This increase in $[Ca^{2+}]_i$ was parallel to the enhancement of NO production; in fact, the release of NO was significantly higher in differentiating cells in comparison with the controls from day 14 of induction onwards (controls: time $0 = 103.87 \pm 6.45$ nmol NO/mg protein; day $14 = 108.31 \pm 7.11$ nmol NO/mg protein; day $21 = 111.27 \pm 6.89$ nmol NO/mg protein; day $28 = 109.68 \pm 7.02$ nmol NO/mg protein. Differentiated: time $0 = 105.78 \pm 7.32$ nmol NO/mg protein; day $14 = 120.36 \pm 7.96$ nmol NO/mg protein; day $21 = 148.96 \pm 8.92$ nmol NO/mg protein; day $28 = 159.45 \pm 9.08$ nmol NO/mg protein) (Fig. 6).

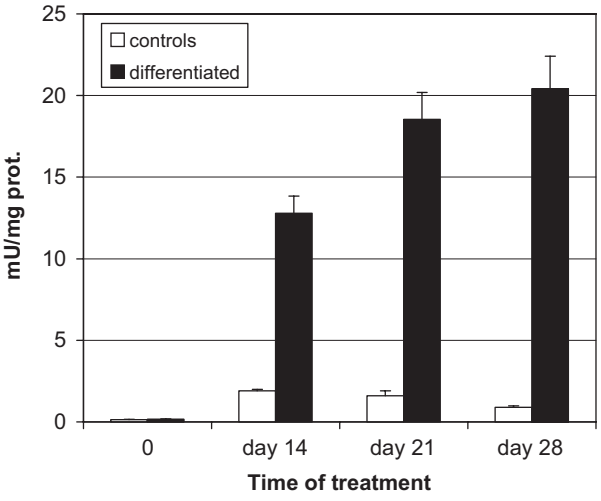

Fig. 4. Alkaline phosphatase (ALP) activity assay in human PDL-MSCs cultured in osteogenic medium (differentiated) with respect to cells treated with culture medium alone (controls). The means $\pm$ S.D. are shown. At days 14, 21 and 28 treated cells vs. controls, $P < 0.001$.

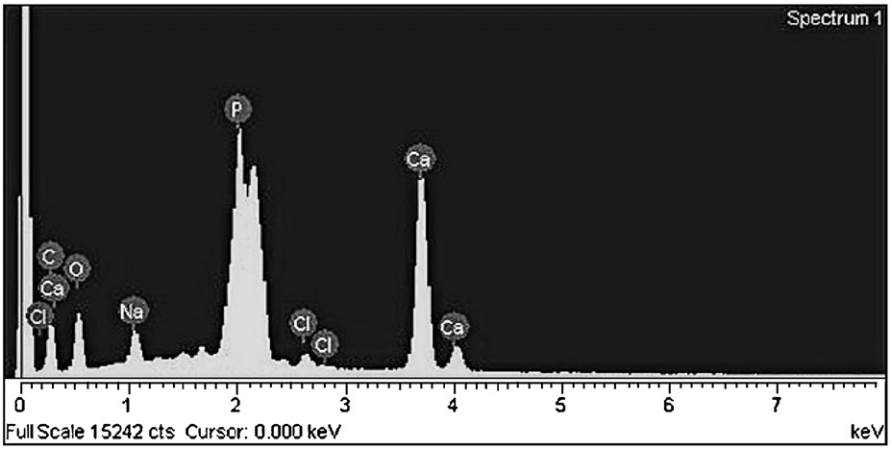

Fig. 3. Results of the energy dispersive X-ray microanalysis: mineralized deposits containing calcium and phosphorus as demonstrated by characteristic EDAX patterns were frequently observed in areas resembling the bone-like nodules.

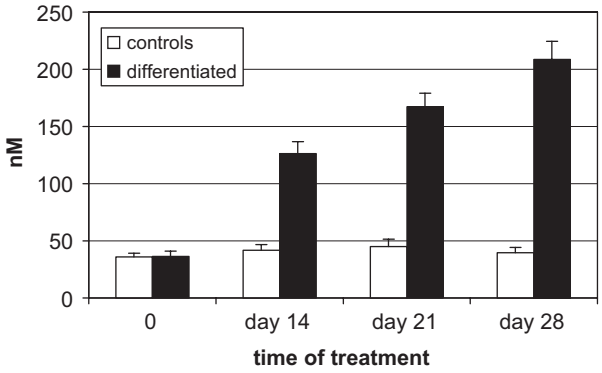

Fig. 5. $[Ca^{2+}]_i$ in human PDL-MSCs cultured in osteogenic medium (differentiated) with respect to cells treated with culture medium alone (controls). The means $\pm$ S.D. are shown. At days 14, 21 and 28 treated cells vs. controls, $P<0.001$.

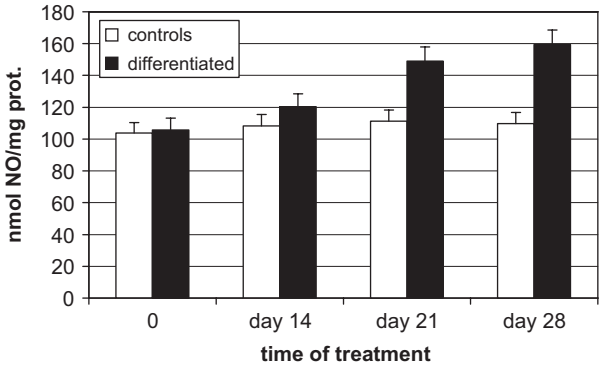

Fig. 6. NO produced by human PDL-MSCs cultured in osteogenic medium (differentiated) with respect to cells treated with culture medium alone (controls). The means $\pm$ S.D. are shown. At day 14 treated cells vs. controls, $P<0.005$. At days 21 and 28 treated cells vs. controls, $P<0.001$.

Discussion

Periodontal diseases are chronic inflammatory diseases of the attachment structures of the teeth and are a major cause of tooth loss in adults and one of the most prevalent forms of bone pathology in humans, thus representing an important public health burden worldwide. While, some minor regeneration of the periodontium may be seen in the early phases, once the disease becomes established then spontaneous regeneration does not occur without therapeutic intervention (Bartold et al., 2000). A primary objective in the treatment of such diseases is the regeneration of mineralized and soft connective tissues. As these tissues are of mesenchymal origin, we focused our attention on adult MSC expanded *ex vivo* from human PDL.

Previously, *in vitro* osteogenesis from adult stem cells has been performed by using bone marrow-derived MSC (Donzelli et al., 2007), however, the method of cell collection is inconvenient and invasive. Attempts to find new sources of stem cells able to differentiate into osteogenic lineages have been investigated. Previous findings by our group showed that human PDL contains a population of multipotent postnatal stem cells that can be isolated and largely expanded *in vitro*, thus providing a reservoir of stem cells from an accessible tissue resource (Trubiani et al., 2005). In this context, our aim was to study the osteogenic differentiation of human PDL-MSCs cultured in the presence of β-glycerophosphate, dexamethasone and ascorbic acid using both morphological and biochemical techniques. The mesenchymal identity of isolated cells was determined by the presence of surface markers.

Our results indicate that the adherent cells expanded *ex vivo* from the PDL are mesenchymal cells that, under certain conditions, can differentiate into bone-forming osteoblasts.

In fact, these PDL-MSCs, when cultured in an osteoconductive medium, have an osteogenic differentiation *in vitro*, resulting in the appearance of active osteoblasts together with the formation of calcified deposits and the increase in ALP activity, as previously shown also in MSC populations derived from bone marrow and dental pulp (Shi and Gronthos, 2003; Gronthos et al., 2000). The morphology of the predominant cell type had a polygonal appearance, postulated by some investigators to reflect an osteoblast-like phenotype (Murata et al., 2004).

The presence of calcium deposits in the extracellular matrix was demonstrated by both alizarin red staining and EDAX microanalysis. As regards the $[Ca^{2+}]_i$, our data are in agreement with previous studies reporting that, under mineralization conditions, cells release calcium from their intracellular stores, and this release can be transduced into an intracellular response (Lundgren et al., 2001). Calcium signalling is known to have a central role in many aspects of osteoblast proliferation and differentiation (Zayzafoon, 2006). One of the effects of this increase in $[Ca^{2+}]_i$ could be the stimulation of eNOS activity. In fact, the activity of the eNOS is primarily regulated at a post-translational level by changes in the free intracellular calcium $[Ca^{2+}]_i$ concentration, which binds to calmodulin associated with the enzyme to induce a conformational change that increases catalytic activity.

Previous studies have demonstrated that NO-dependent signalling via eNOS is important in

regulating several aspects of osteoblast biology including growth, differentiation, recruitment and extracellular matrix synthesis (Aguirre et al., 2001). It has been previously shown that osteoblast differentiation and maintenance of bone mass are impaired in ecNOS gene knockout mice (Aguirre et al., 2001; Armour et al., 2001). However, the molecular mechanisms through which NO influences osteogenesis remain unclear.

Since our results show that the increase in NO production was parallel to the enhancement of alkaline phosphatase activity, we could hypothesize that NO serves as a positive regulator of ALP activity, in agreement with previous data obtained in rat odontoblasts and pulp cells during dentin repair. In the rat it has been demonstrated that pulp MSCs treated with an NO donor show enhanced ALP activity and mineralized nodule formation (Mei et al., 2007).

In conclusion, our data show an involvement of NO in the osteogenesis of human PDL-MSCs, thus suggesting that local reimplantation of *ex vivo* expanded cells in conjugation with an NO donor could represent a promising approach for bone regenerative procedures. In a tissue engineering approach for bone augmentation, it would be an advantage to use autologous stem cells from a dental site, thereby reducing the morbidity related to bone harvesting from, for example, the iliac crest. Moreover, unpublished findings of our group demonstrated that PDL-MSCs could also be isolated from the coronal portion of the PDL, without extracting teeth, by scraping the periodontal fibers of the alveolar crest group and the horizontal group, thus providing a readily accessible source of MSCs for periodontal tissue regeneration. The simple way in which MSCs can be obtained from the PDL and their capacity to proliferate and to differentiate make this source particularly feasible for clinical application in restorative surgery. Further studies are still required in order to better clarify the molecular mechanisms activated by NO during PDL-MSCs osteogenesis.

Acknowledgments

The authors wish to thank Dr. Stefano Squarzoni, ITOI, CNR, Unit of Bologna, c/o IOR, Bologna, Italy, for the microanalysis results and Dr. Ray Pizzuto for the English revision of the article. This work was supported by Grants FIRB-RBNE01N4Z9_003 and PRIN 2004111320_004 from the Ministero dell' Università e della Ricerca Scientifica e Tecnologica, Italy and RSA Grants from Università di Chieti-Pescara e Politecnica delle Marche, Italy.

References

Aguirre J, Buttery L, O'Shaughnessy M, Afzal F, Fernandez de Marticorena I, Hukkanen M, et al. Endothelial nitric oxide synthase gene-deficient mice demonstrate marked retardation in postnatal bone formation, reduced bone volume, and defects in osteoblast maturation and activity. Am J Pathol 2001;158: 247–57.

Armour KE, Armour KJ, Gallagher ME, Gödecke A, Helfrich MH, Reid DM, et al. Defective bone formation and anabolic response to exogenous estrogen in mice with targeted disruption of endothelial nitric oxide synthase. Endocrinology 2001;142:760–6.

Bartold PM, McCulloch CA, Narayanan AS, Pitaru S. Tissue engineering: a new paradigm for periodontal regeneration based on molecular and cell biology. Periodontol 2000;24:253–69.

Beertsen W, McCulloch CA, Sodek J. The periodontal ligament: a unique, multifunctional connective tissue, Periodontol 2000/1997;13:20–40.

Boyko A, Melcher AH, Brunette DM. Formation of new periodontal ligament by periodontal ligament cells implanted *in vivo* after culture *in vitro* A preliminary study of transplanted roots in the dog. J Periodontal Res 1981;16:73–88.

Bradford MM. A rapid and sensitive method for the quantitation of microgram quantities of protein utilising the principle of protein-dye binding. Anal Biochem 1976;72:248–54.

Chamberlain JR, Schwarze U, Wang PR, Hirata RK, Hankenson KD, Pace JM, et al. Gene targeting in stem cells from individuals with osteogenesis imperfecta. Science 2004;303:1198–201.

Chaudhary LR, Hofmeister AM, Hruska KA. Differential growth factor control of bone formation through osteoprogenitor differentiation. Bone 2004;34: 402–11.

Crevensten G, Walsh AJ, Ananthakrishnan D, Page P, Wahba GM, Lotz JC, et al. Intervertebral disc cell therapy for regeneration: mesenchymal stem cell implantation in rat intervertebral discs. Ann Biomed Eng 2004;32:430–4.

Donzelli E, Salvadè A, Mimo P, Viganò M, Morrone M, Papagna R, et al. Mesenchymal stem cells cultured on a collagen scaffold: in vitro osteogenic differentiation. Arch Oral Biol 2007;52:64–73.

Gage FH. Mammalian neural stem cells. Science 2000; 287:1433–8.

Gould TR, Melcher AH, Brunette DM. Migration and division of progenitor cell populations in periodontal ligament after wounding. J Periodontal Res 1980;15: 20–42.

Green LC, Wagner DA, Glogowski J, Skipper PL, Wishnok JS, Tannenbaum SR. Analysis of nitrate, nitrite and [^{15}N] nitrate in biological fluids. Ann Biochem 1982; 126:131–8.

Grinnemo KH, Mannsonn A, Delgren G, Klingberg D, Wardell E, Drvota V, et al. Xenoreactivity and engraftment of human mesenchymal stem cells

transplanted into infracted rat myocardioum. J Thorac Cardiovasc Surg 2004;127:1293–300.

Gronthos S, Mankani M, Brahim J, Robey PG, Shi S. Postnatal human dental pulp stem cells (DPSCs) in vitro and in vivo. Proc Natl Acad Sci USA 2000;97: 13625–30.

Grynkiewicz G, Poenie M, Tsien RY. A new generation of Ca^{2+} indicators with greatly improved fluorescence properties. J Biol Chem 1985;260:3440–50.

Helfrich MH, Evans DE, Grabowski PS, Pollock JS, Ohshima H, Ralston SH. Expression of nitric oxide synthase isoforms in bone and bone cell cultures. J Bone Miner Res 1997;12:1108–15.

Ivanovski S, Gronthos S, Shi S, Bartold PM. Stem cells in the periodontal ligament. Oral Dis 2006;12:358–63.

Jiang Y, Jahagirdar BN, Reinhardt RL, Schwartz RE, Keene CD, Ortiz-Gonzales XR, et al. Pluripotency of mesenchymal stem cells derived from adult marrow. Nature 2002;418:41–9.

Lundgren T, Nilsson M, Ritchie HH, Linde A. Junctional proteins and Ca^{2+} transport in the rat odontoblast-like cell line MRPC-1. Calcif Tissue Int 2001;68:192–201.

Mei YF, Yamaza T, Atsuta I, Danjo A, Yamashita Y, Kido MA, et al. Sequential expression of endothelial nitric oxide synthase, inducible nitric oxide synthase, and nitrotyrosine in odontoblasts and pulp cells during dentin repair after tooth preparation in rat molars. Cell Tissue Res 2007;328:117–27.

Morishita M, Yamamura T, Shimazu A, Bachchu AH, Iwamoto Y. Estradiol enhances the production of mineralized nodules by human periodontal ligament cells. J Clin Periodontol 1999;26:748–51.

Murata H, Tanaka H, Taguchi T, Shiigi E, Mizokami H, Sugiyama T, et al. Dexamethasone induces human spinal ligament derived cells toward osteogenic differentiation. J Cell Biochem 2004;92:715–22.

Narayanan K, Ramachandran A, Hao J, He G, Park KW, Cho M, et al. Dual functional roles of dentin matrix protein 1. J Biol Chem 2003;278:17500–8.

Pierdomenico L, Bonsi L, Calvitti M, Rondelli D, Arpinati M, Chirumbolo G, et al. Multipotent mesenchymal stem cells with immunosoppressive activity can be easily isolated from dental pulp. Transplantation 2005;80:836–42.

Prockop DJ. Marrow stromal cells as stem cell for nonhematopoietic tissues. Science 1997;276:71–4.

Ralston SH. Nitric oxide and bone: what a gas!. Br J Rheumatol 1997;36:831–8.

Rao GHR. Measurement of ionized calcium in normal human blood platelets. Anal Biochem 1988;169:400–4.

Riancho JA, Salas E, Zarrabeitia MT, Olmos JM, Amado JA, Fernandez-Luna JL, et al. Expression and functional role of nitric oxide synthase in osteoblast-like cells. J Bone Miner Res 1995;10:439–46.

Salter M, Knowles RG, Moncada S. Widespread tissue distribution, species distribution and changes in activity of Ca(2+)-dependent and Ca(2+)-independent nitric oxide synthases. FEBS Lett 1991;291:145–9.

Seo BM, Miura M, Gronthos S, Bartold PM, Batouli S, Brahim J, et al. Investigation of multipotent postnatal stem cells from human periodontal ligament. Lancet 2004;364:149–55.

Shi S, Gronthos S. Perivascular niche of postnatal mesenchymal stem cells in human bone marrow stromal fibroblasts. Transplantation 2003;63:696–704.

Spradling A, Drummond-Barbosa D, Kai T. Stem cells find their niche. Nature 2001;414:98–104.

Sugaya K. Potential use of stem cells in neuroreplacement therapies for neurodegenerative diseases. Int Rev Cytol 2003;228:1–30.

Toma JG, Akhavan M, Fernandes KJ, Barnabe-Heider F, Sadikot A, Kaplan DR, et al. Isolation of multipotent adult stem cells from the dermis of mammalian skin. Nat Cell Biol 2001;3:778–84.

Trubiani O, Di Primio R, Traini T, Pizzicannella J, Scarano A, Piattelli A, et al. Morphological and cytofluorimetric analysis of adult mesenchymal stem cells expanded *ex vivo* from periodontal ligament. Int J Immunopathol Pharmacol 2005;18:213–21.

Zayzafoon M. Calcium/calmodulin signaling controls osteoblast growth and differentiation. J Cell Biochem 2006;97:56–70.